PAPER

Check for updates

Synthesis and characterization of silicone polyurea and mechanical properties improvement through interfacial reaction

Yanru Chen, [ID] * Ke Yang, Hanhai Dong, Hongyu Niu, Quanguo Wang and Qingli Cheng

Silicone polyurea typically exhibits inferior mechanical properties due to the microphase separation between the siloxane and polyurea segments. To address this issue, we propose a method to enhance the mechanical properties through interfacial reactions. The mechanical properties and microphase separation of silicone polyurea we synthesized were studied. And poly(isobutene-*alt*-maleic anhydride) (PBAM) and γ-aminopropyl triethoxysilane (KH550) which are capable of interfacial reactions were respectively introduced into polyurea and siloxane segments to reduce the degree of microphase separation and enhance the mechanical properties of silicone polyurea. The mechanism behind the improvement was elucidated through experimental results. FT-IR spectra confirmed that the maleic anhydride groups in PBAM and the amino groups in KH550 undergo rapid reactions. Additionally, it was observed that the rapid interaction of PBAM and KH550 at the interface made interfacial tension decrease fast through the pendant-drop method. Stability analysis and light microscope observations revealed that PBAM and KH550 can stabilize the two-phase interface, forming stable droplets within the mixture. Scanning electron microscopy (SEM) observations indicated a reduction in the degree of microphase separation in the silicone polyurea. Consequently, the introduction of PBAM and KH550 decreases interfacial tension and the dispersion size of the silicone phase within the carbon phase, thereby reducing the degree of microphase separation and enhancing the mechanical properties of the silicone polyurea.

1 Introduction

Polyureas are a class of polymer elastomers synthesized from isocyanates and amine compounds. Due to their fast reaction rate and strong adhesion, they are often used as protective coatings.[1–6] Silicone resins are widely applied in fields such as the construction industry, automotive and transportation industry, electronics industry and aerospace due to their unique advantages such as high weather resistance and thermal stability.[7–12] The copolymerization of silicone materials and polyurea elastomers can combine the advantages of both, which has attracted much attention in the field in recent years.[13–15] In previous work, silicone polyurea exhibited microphase separation due to the large difference of solubility parameters between polyurea (urea groups: 45.6 $(J\ cm^{-3})^{1/2}$) and silane (PDMS: 15.6 $(J\ cm^{-3})^{1/2}$).[16,17] Zhang *et al.* utilized the microphase separation of polyurea and silane to prepare materials with micro- and nano-scale roughness for the construction of hydrophobic surfaces.[18] However, the microphase separation of polyurea and silane has negative effects on

the mechanical properties.[19] This is due to the difference in solubility parameters of the two phases making the interfacial interaction force weak. Consequently, the material exhibited poor stress transfer capabilities and became prone to interfacial fracture under tensile loading.

Adding compatibilizers in polymer materials is a common method to reduce microphase separation and enhance mechanical properties.[20–23] Singh has reviewed the research on the compatibilization of polypropylene (PP) and acrylonitrile–butadiene–styrene (ABS) blends.[24] PP possesses high tensile strength but is brittle at low temperatures, while ABS has good toughness but lower tensile strength and elongation at break. Compatibilized blends of PP and ABS can simultaneously enhance their tensile strength, impact strength, toughness, and elongation at break. Compatibilizers can improve the adhesion at the polymer interface, thereby increasing the compatibility of the blend. The microstructure of materials affects their overall properties, and the morphology, domain size, and dispersion state of the blend have a significant impact on mechanical strength. Maleic anhydride copolymers (such as styrene-grafted maleic anhydride and polypropylene-grafted maleic anhydride) are commonly used compatibilizers.[25,26] Belyamani used a styrene–ethylene–butylene–styrene

SINOPEC Research Institute of Safety Engineering Co., Ltd., Qingdao, 266100, People's Republic of China. E-mail: chenyr.qday@sinopec.com; Tel: +86 532 83786462

copolymer grafted with maleic anhydride as a compatibilizer, studying the effects of compatibilizer concentration, reactivity of maleic anhydride groups, and styrene content on compatibilization efficiency.[27] Scanning electron microscopy analysis showed that it reduced phase separation, resulting in a more uniform fracture surface. Kameshwari investigated the impact of styrene–maleic anhydride copolymer (SMA) as a compatibilizer on the properties of polycarbonate (PC)/acrylonitrile–butadiene–styrene (ABS) blends.[28] PC/ABS blends with SMA as a compatibilizer showed significant improvements in tensile properties, and impact strength was higher than that of pure ABS. SEM images revealed that the dispersion of the compatibilized blend was more uniform, indicating that the SMA compatibilizer played a role in reducing microphase separation between the PC and ABS phases. However, there are few researches on compatibilizers for reducing the microphase separation of silicone polyurea.

In this paper, we incorporated PBAM and KH550 into the synthesis process of silicone polyurea to mitigate microphase separation and enhance the material's mechanical properties. PBAM contains a large amount of maleic anhydride which can react with KH550 at the interface. And the polymer PBAM–KH550 produced after reaction with KH550 has both carbon chain and silicon chain, which can improve the interaction force between the two phases. Our research delves into the mechanical properties and microphase separation of the synthesized silicone polyurea, elucidating the mechanism by which PBAM–KH550 diminishes phase separation and strengthens mechanical attributes. FT-IR confirmed the rapid reaction between the maleic anhydride groups in PBAM and the amino groups in KH550. The pendant-drop method demonstrated a swift decrease in interfacial tension due to the rapid interaction between PBAM and KH550 at the interface. Stability analyses and light microscope observations confirmed that PBAM and KH550 can stabilize the two-phase interface, leading to the formation of stable droplets within the mixture. SEM observations revealed a reduction in microphase separation within the silicone polyurea. Consequently, the integration of PBAM and KH550 reduces interfacial tension and the dispersion size of the silicone phase within the carbon phase, thereby lessening microphase separation and enhancing the mechanical properties of the silicone polyurea. This approach demonstrates a promising strategy for improving the performance of silicone polyurea materials through targeted interfacial interactions.

2 Experimental section

2.1 Materials

Poly(isobutene-*alt*-maleic anhydride) (PBAM) was sourced from Sigma-Aldrich Reagent Corporation. γ-Aminopropyl triethoxysilane (KH550) and silicone oil were procured from Macklin Biochemical Technology Co., Ltd in Shanghai, China. *N,N*-Dimethylacetamide (DMAc), ethyl acetate and xylene were acquired from Sinopharm Chemical Reagent Co., Ltd, Shanghai, China. Isophorone diisocyanate (IPDI) and polyether amine (D2000, D230, T403) were obtained from Aladdin
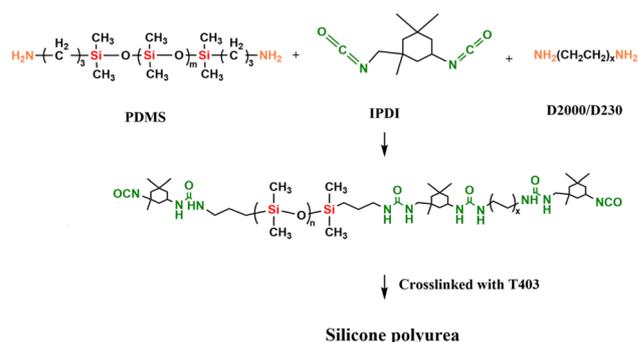

Fig. 1 Synthesis of silicone polyurea.

Biochemical Technology Co., Ltd. Shanghai, China. All polydimethylsiloxane (PDMS) was purchased from Inoac Corporation. All materials are analytical reagent grade and used in their received state, without any further treatment.

2.2 Characterization methods

Infrared spectra were recorded using a Mettler 702L online infrared monitoring system at ambient temperature. Thermogravimetric analysis (TGA) curves were obtained with a Netzsch STA 449 instrument, scanning from 40 °C to 800 °C under a nitrogen atmosphere, with a heating rate of 10 K min^{-1}. Fourier-transform infrared (FT-IR) spectra were acquired using the attenuated total reflectance (ATR) method over the wavenumber range of 4000 to 400 cm^{-1} with a Bruker Tensor 27 spectrometer. The interfacial tension and reactivity were assessed using the drop tracker method with a Dataphysics OCA25 instrument from Germany, employing DMAc as the ambient phase and silicone oil as the droplet phase. The stability of the mixtures was evaluated using an optical analyzer, the Dataphysics MultiScan MS 20 from Germany, with the Turbiscan stability index (TSI) indicating the degree of instability, where higher TSI values suggest less stability. Optical microscope images were captured with an XFL-500 L microscope from VIYEE Photoelectric, China. Morphology observations and energy dispersive spectra (EDS) were conducted using a JEOL JCM-7000 scanning electron microscope (SEM). The

Table 1 Formulas of silicone polyurea

Sample	IPDI/g	D2000/g	PDMS/g	D230/g	T403/g
Polyurea	2.75	7.00	0.00	1.83	0.14
PUA–Si 2500 Da-1	2.75	5.50	2.20	1.83	0.14
PUA–Si 2500 Da-2	2.75	4.00	3.75	1.83	0.14
PUA–Si 2500 Da-3	2.75	3.00	5.00	1.83	0.14
PUA–Si 2500 Da-4	2.75	0.00	8.75	1.83	0.14
PUA–Si 5000 Da-1	2.75	6.12	2.20	1.83	0.14
PUA–Si 5000 Da-2	2.75	5.50	3.75	1.83	0.14
PUA–Si 5000 Da-3	2.75	5.00	5.00	1.83	0.14
PUA–Si 5000 Da-4	2.75	3.50	8.75	1.83	0.14
PUA–Si 1000 Da-1	2.75	2.60	2.20	1.83	0.14
PUA–Si 7000 Da	2.75	6.41	2.20	1.83	0.14
PUA–Si 10000 Da	2.75	6.56	2.20	1.83	0.14

mechanical properties were tested 3 times on a universal testing machine, the i-Strentek 1510 from Labthink, China, with samples cut into a dumbbell shape for testing.

2.3 Synthesis

The schematic synthesis of silicone polyurea is depicted in Fig. 1. IPDI, D2000 and PDMS were measured according to the quantities listed in Table 1 and introduced into a beaker containing 20 g of ethyl acetate and 10 g of xylene as solvents. Once the reactants were thoroughly mixed, D230 and T403 were added in sequence. The reaction mixture was then transferred into a tetrafluoroidal mold after being stirred for 3 minutes. The silicone polyurea was allowed to cure and dry at room temperature for five days before being subjected to further testing.

The preparation of silicone polyurea incorporating PBAM–KH550 follows a similar procedure. IPDI and D2000 were measured and placed into a beaker with 20 g of ethyl acetate and 10 g of xylene as solvents. After complete mixing, a solution of PBAM in DMAc was added. Once PDMS and KH550 were uniformly mixed, this mixture was added to the beaker. Subsequently, D230 and T403 were added in order. The reaction solution was poured into a tetrafluoroidal mold after 3 minutes of stirring. The curing and drying process was identical to the one described above.

The synthesis procedure for PBAM–KH550 is detailed as follows: 1.312 g of PBAM is reacted with 0.942 g of KH550 (with a molar ratio of maleic anhydride to amino groups of 1 : 1) in DMAc as the solvent. After the solvent evaporates, a solid powder is obtained, which is then subjected to TGA testing.

3 Results and discussion

3.1 Synthesis and properties of silicone polyureas

A series of silicone polyurea materials were synthesized, and their structures were characterized and properties were tested for the subsequent application of KH550 and PMAB in this silicone polyurea material.

Firstly, the silicone polyurea materials were characterized by FT-IR. As shown in Fig. 2, the peak at 1626 cm^{-1} corresponds to C=O stretching vibration of polyurea. The peak at 3300 cm^{-1} is attributed to N–H stretching vibration of secondary amine. The peaks observed at 2976 cm^{-1} and 1259 cm^{-1} are associated with C–H stretching vibration and bending vibration of the methyl groups in PDMS. The peak at 797 cm^{-1} and 1017 cm^{-1} are indicative of the Si–C and Si–O–Si stretching vibration, respectively. As the PDMS content in silicone polyurea materials increased, the intensity of the peaks at 2976 cm^{-1}, 797 cm^{-1} and 1017 cm^{-1} correspondingly intensified. These FT-IR results provide confirmatory evidence of the successful synthesis of the silicone polyurea materials.

The thermal decomposition characteristics of silicone polyurea materials were investigated. TGA and DTG curves for both polyurea and silicone polyurea are presented in Fig. 3. Fig. 3a illustrates that the initial thermal decomposition temperature (corresponding to a 5% weight loss) for silicone polyurea synthesized with varying amounts of PDMS (2500 Da) is
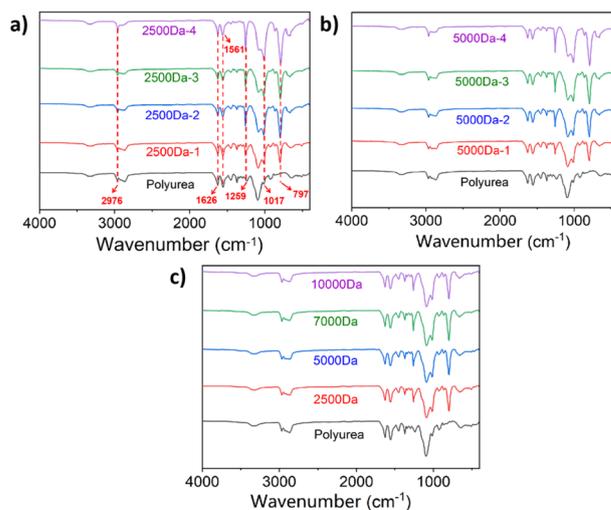

Fig. 2 FT-IR spectra of silicone polyurea with different dosage and molecular weight of silicone.

approximately 300 °C, attributed to the decomposition of carbon chains. The weight loss within the temperature range of 400–600 °C is associated with the decomposition of the silicone segments. An increase in silicone content within the polyurea leads to a slower decomposition rate for the samples in the 400–600 °C range. By 600 °C, the silicone polyurea is completely decomposed. The decomposition behavior of silicone polyurea synthesized with PDMS of 5000 Da molecular weight is analogous, as shown in Fig. 3b. The thermal decomposition performance of silicone polyurea with PDMS of different molecular weights was also examined. As depicted in Fig. 3c, within the temperature range of 400–600 °C, the degree of thermal decomposition decreases with increasing molecular weight of PDMS. This reduction in decomposition is due to the higher molecular weight of PDMS, which enhances the interaction between the silicone segments and the polyurea chains.

The mechanical properties of the silicone polyureas were depicted in Fig. 4, where it is evident that both the molecular weight and the quantity of PDMS influence these properties. As observed in Fig. 4a, the tensile strength and the elongation at break of silicone polyureas prepared with PDMS of 2500 Da molecular weights tend to decrease as the PDMS content increases. This reduction is attributed to the increased silicone content disrupting the microstructure of the pure polyurea, consequently leading to a decline in the mechanical properties of the silicone polyureas.[17] Fig. 4b shows a similar trend for silicone polyureas prepared with PDMS of 5000 Da molecular weight. An increase in molecular weight is associated with improved tensile strength and elongation at break in silicone polyureas. This improvement is attributed to the fact that, with a constant amount of PDMS, the degree of microphase separation remains relatively consistent. Consequently, the increase in molecular weight enhances the mechanical properties of the silicone polyurea.[19] And PUA–Si 7000 Da has better mechanical properties than pure polyurea. In this formula of silicone polyurea, when the molecular weight of silicone is greater than
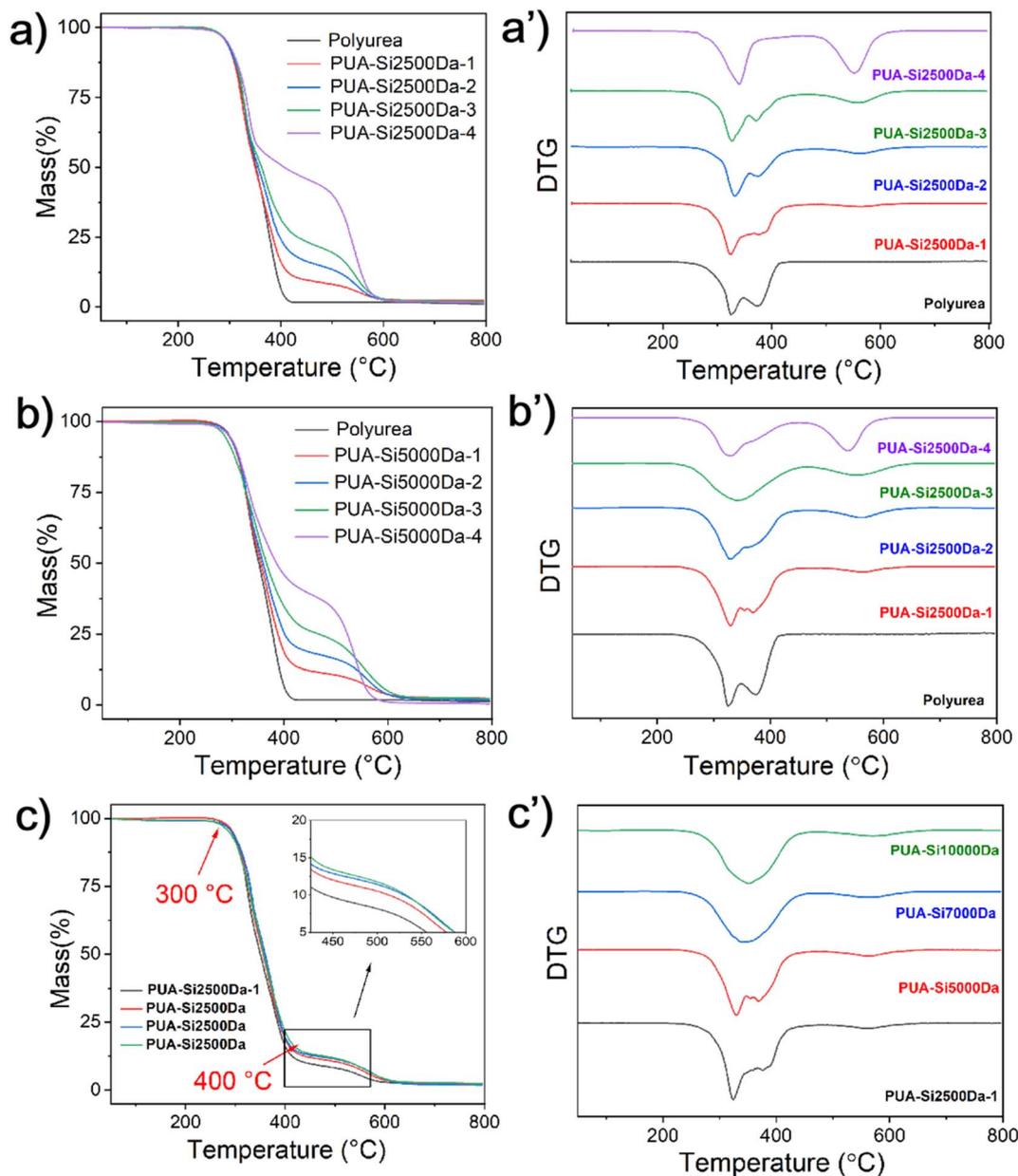
Fig. 3 TGA (a–c) and DTG (a′–c′) curves of polyurea and silicone polyurea with different dosage and molecular weight of silicone.

7000 Da, the contribution of molecular weight to mechanical properties can offset the effect of microphase separation on mechanical properties. The tensile strength and elongation at break of PUA–Si 7000 Da are recorded at 15.3 MPa and 640%, respectively. The cross-section of PUA–Si 7000 Da after being frozen in liquid nitrogen was examined using SEM, as depicted in Fig. 5. The sample displays an uneven cross-section (Fig. 5a), and it is evident that microphase separation occurs, as confirmed by element mapping (Fig. 5d).

3.2 Improving mechanical properties through interfacial reaction

PBAM and KH550 were respectively incorporated in polyurea and siloxane segments on according to the PUA–Si 7000 Da

formulation. This incorporation aimed to facilitate interfacial reactions, as illustrated in Fig. 6. Their stress–strain curves and mechanical properties were subsequently evaluated and are presented in Fig. 7. It was observed that as the content of PBAM and KH550 increased, the tensile strength of the silicone poly-urea also increased progressively. For comparative analysis, separate samples of silicone polyurea with only PBAM and only KH550 added were prepared, and their mechanical properties were tested, as depicted in Fig. 7c and d. The tensile strength of the silicone polyurea with solely PBAM remained largely unchanged. In contrast, the tensile strength and elongation at break of the silicone polyurea with added KH550 decreased with increasing KH550 content. It was concluded that the enhance-ment in the mechanical properties of the silicone polyurea with both PBAM and KH550 was primarily due to the reactions
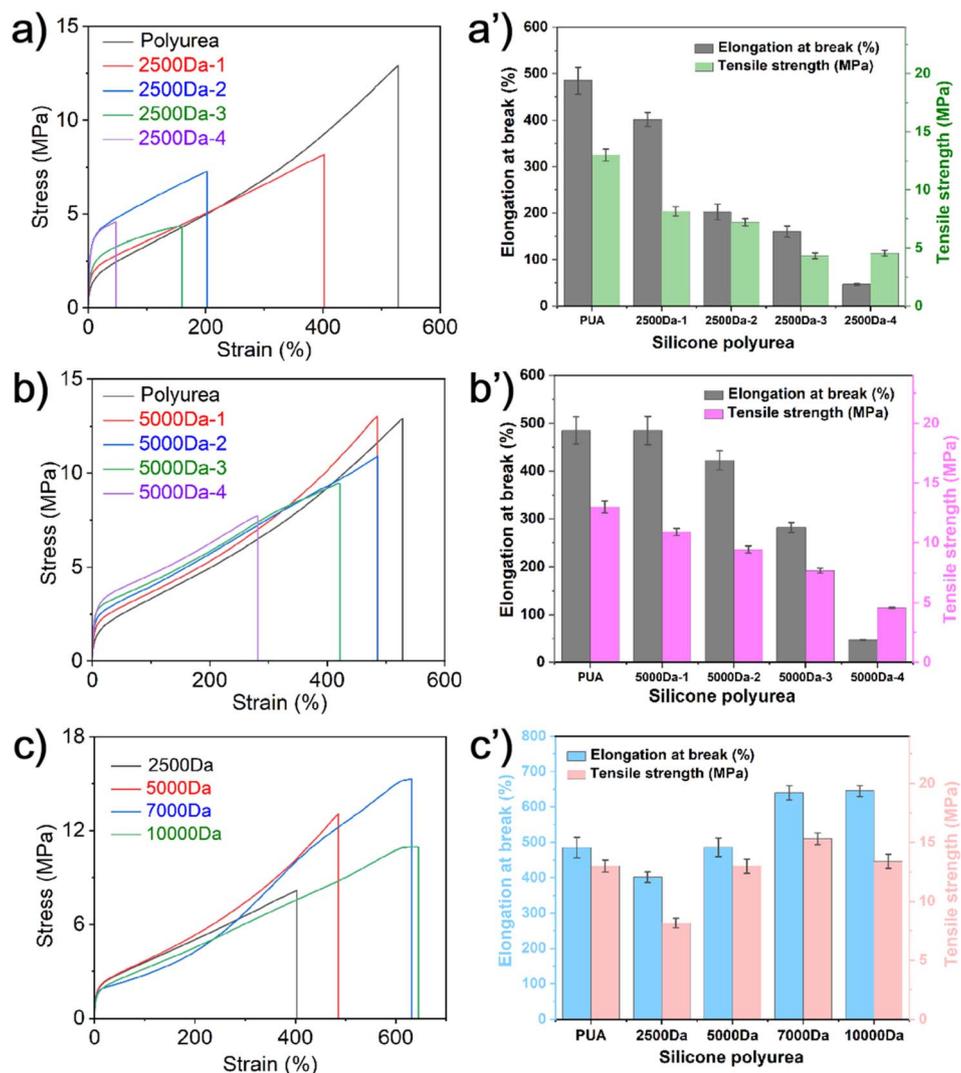
Fig. 4 Mechanical properties of silicone polyurea with different dosage and molecular weight of silicone.
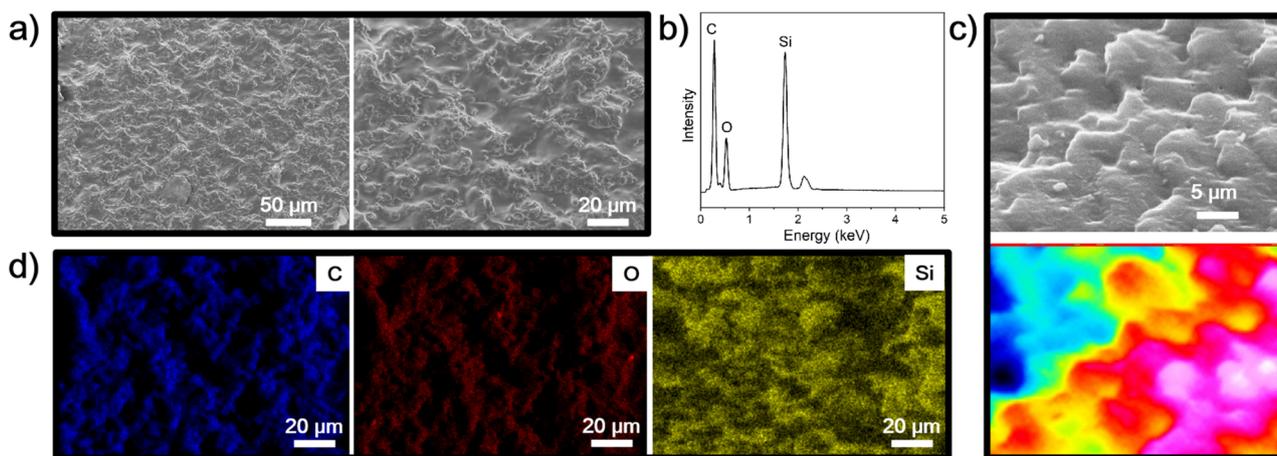

Fig. 5 SEM (a), EDS (b), 3D scanning of SEM (c) and element mapping (d) of PUA–Si 7000 Da.
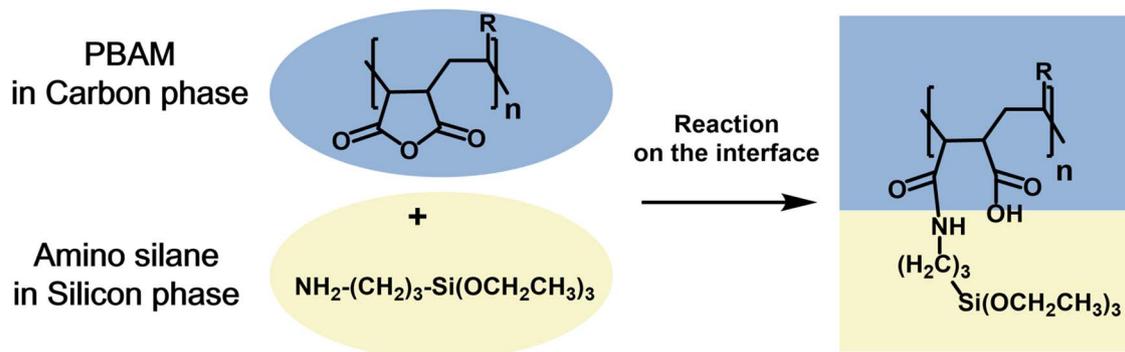
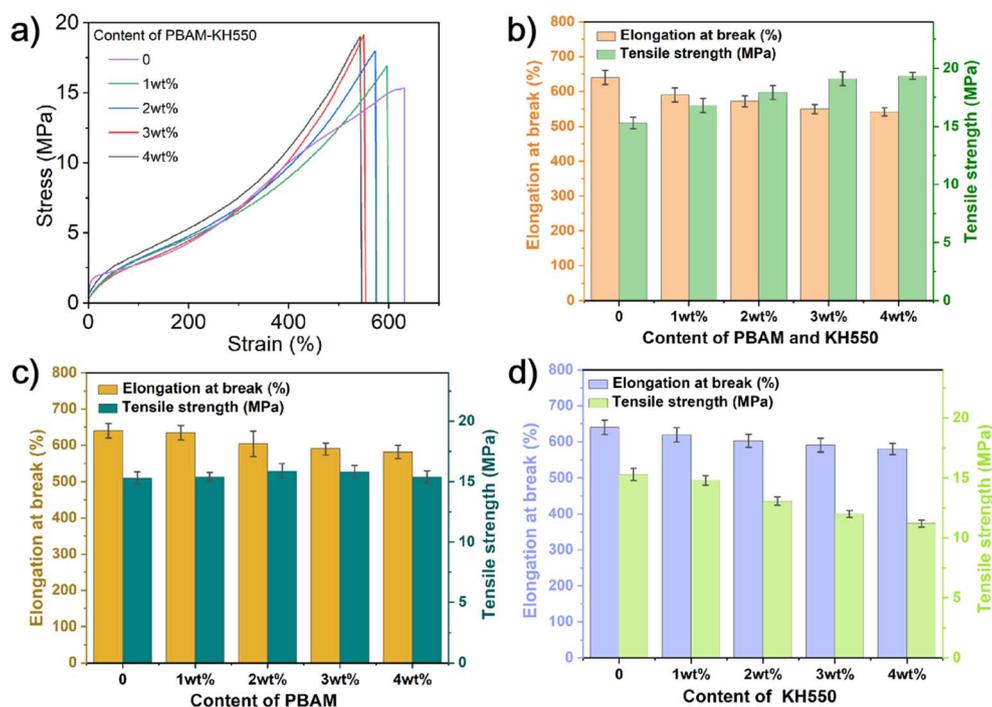Fig. 6 Interfacial reaction of maleic anhydride copolymer and amino silane.

Fig. 7 Stress−strain curves (a) and mechanical properties of silicone polyurea with PBAM−KH550 (b), PBAM (c) and KH550 (d) added respectively.
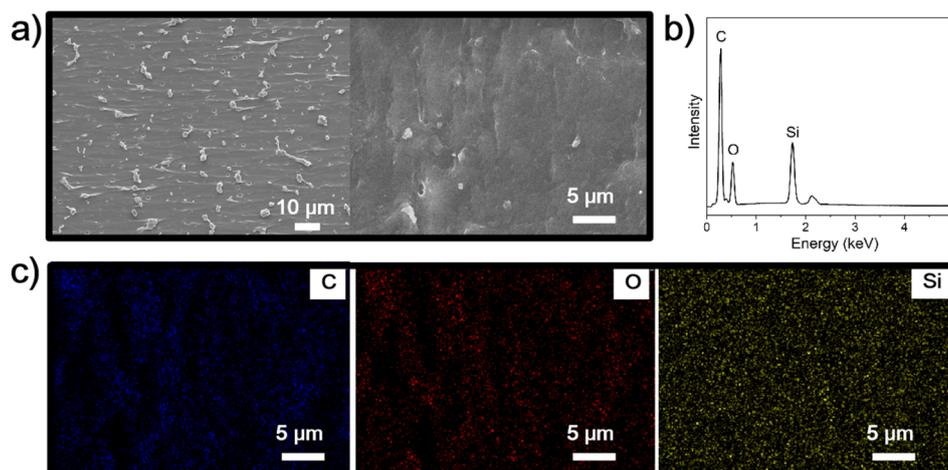

Fig. 8 SEM (a), EDS (b) and element mapping (c) of PUA−Si 7000 Da with PBAM−KH550.
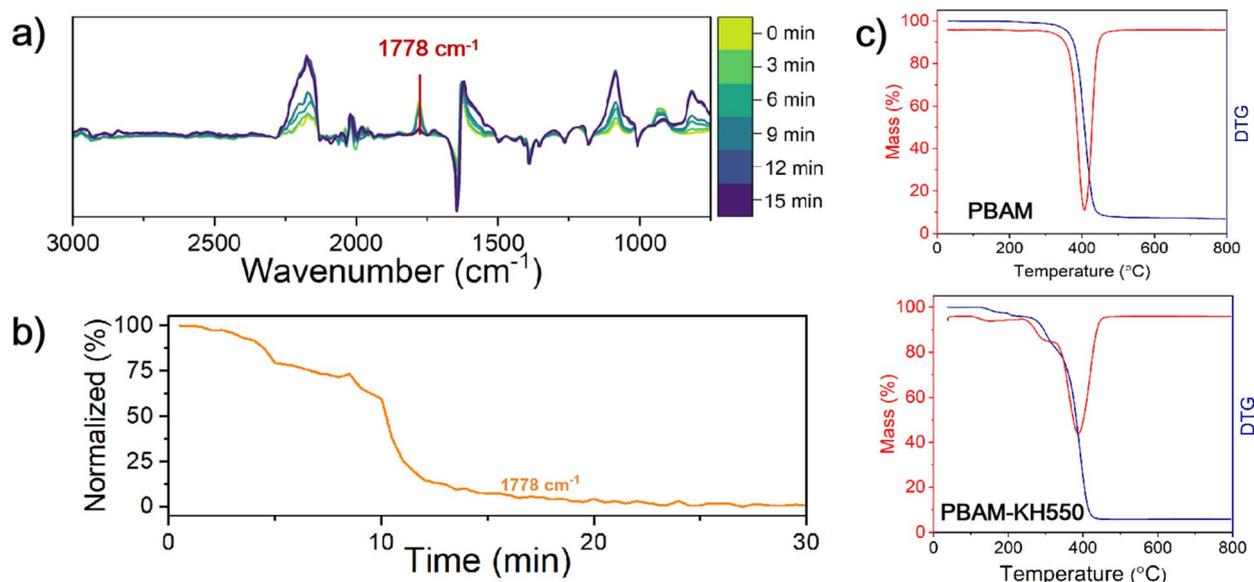
Fig. 9 Online infrared monitoring spectra (a) and trend (b) of PBAM reacting with KH550. (c) TGA curves of PBAM and PBAM–KH550.

occurring at the interface.[29] The cross-sectional morphology of the 3 wt% PBAM and KH550 added sample after freeze fracturing is displayed in Fig. 8. In comparison to the morphology shown in Fig. 6, the cross-section of the material appears flatter after the addition of PBAM and KH550. The elemental distribution is more uniform, and the microscopic phase separation is reduced.

3.3 Mechanism of mechanical properties improvement

Maleic anhydrides are known to react readily with primary amines.[30,31] In this study, the reactivity between maleic anhydride in PBAM and the amino group in KH550 was confirmed using an online infrared monitoring technique. The reaction was carried out at room temperature, with DMAc serving as the solvent. Initially, the infrared spectrum of DMAc was recorded
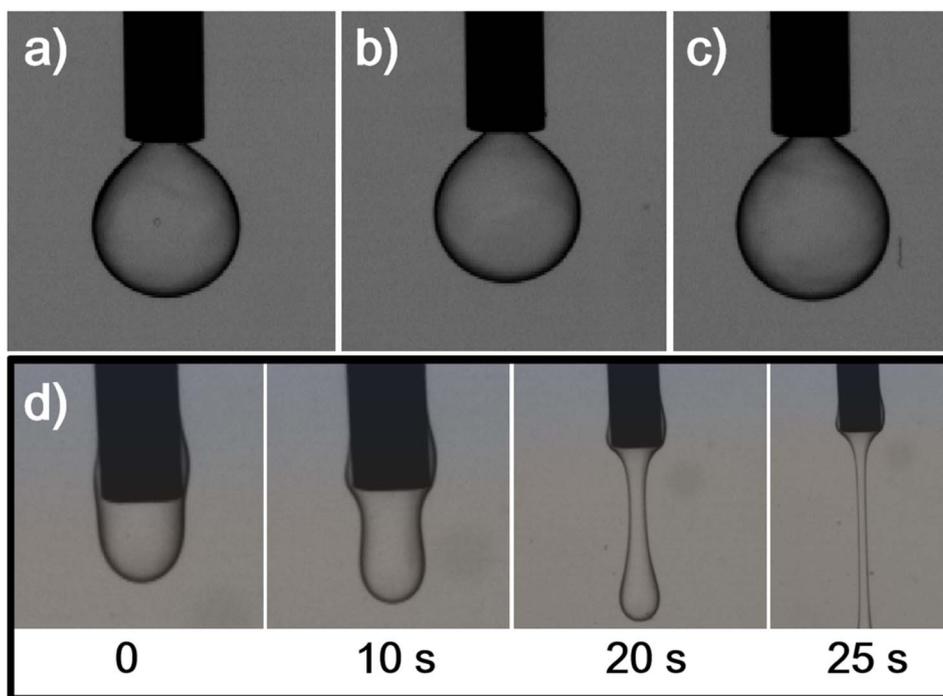

Fig. 10 (a) Interfacial phenomenon between DMAc (droplet) and silicone oil (ambient phase) (b) interfacial phenomenon between DMAc (droplet) and KH550 dissolved in silicone oil (c) interfacial phenomenon between PBAM dissolved in DMAc and silicone oil (d) interfacial phenomenon between PBAM dissolved in DMAc and KH550 dissolved in silicone oil.

to establish a baseline reference. Following this, the infrared spectra of PBAM and the aminosilane DMAc solutions were detected separately to serve as comparative references. Fig. 9a displays the online infrared monitoring spectrum of the reaction process where aminosilane was added to the PBAM solution. The peak at 1778 cm^{-1} corresponded to the C=O stretching vibration of cyclic amide in PBAM. The characteristic absorption peak of PBAM gradually diminishes with the addition of aminosilane, indicating that the aminosilane can rapidly react with the anhydride groups in PBAM.

Additionally, TGA tests were conducted on both PBAM and PBAM–KH550 to evaluate their thermal stability. Fig. 9c presents the results, which show that the initial decomposition temperature (corresponding to a 5% weight loss) for PBAM is 390 °C. In the case of PBAM–KH550, there is only a minor weight loss at the boiling point of KH550, which is 217 °C. This observation further confirms the successful reaction between KH550 and PBAM.

The interfacial reaction characteristics of PBAM and KH550 were investigated using the pendant drop method, as depicted in Fig. 10. Two immiscible solvents, DMAc and silicone oil, were chosen to mimic the polyurea and siloxane segments present in silicone polyurea materials, with DMAc serving as the ambient phase and silicone oil as the droplet phase. Initially, it was observed that silicone oil droplets could stably exist within DMAc. Building on this, we analyzed the interfacial behavior between DMAc (as the droplet phase) and KH550 dissolved in silicone oil, as well as between PBAM dissolved in DMAc and
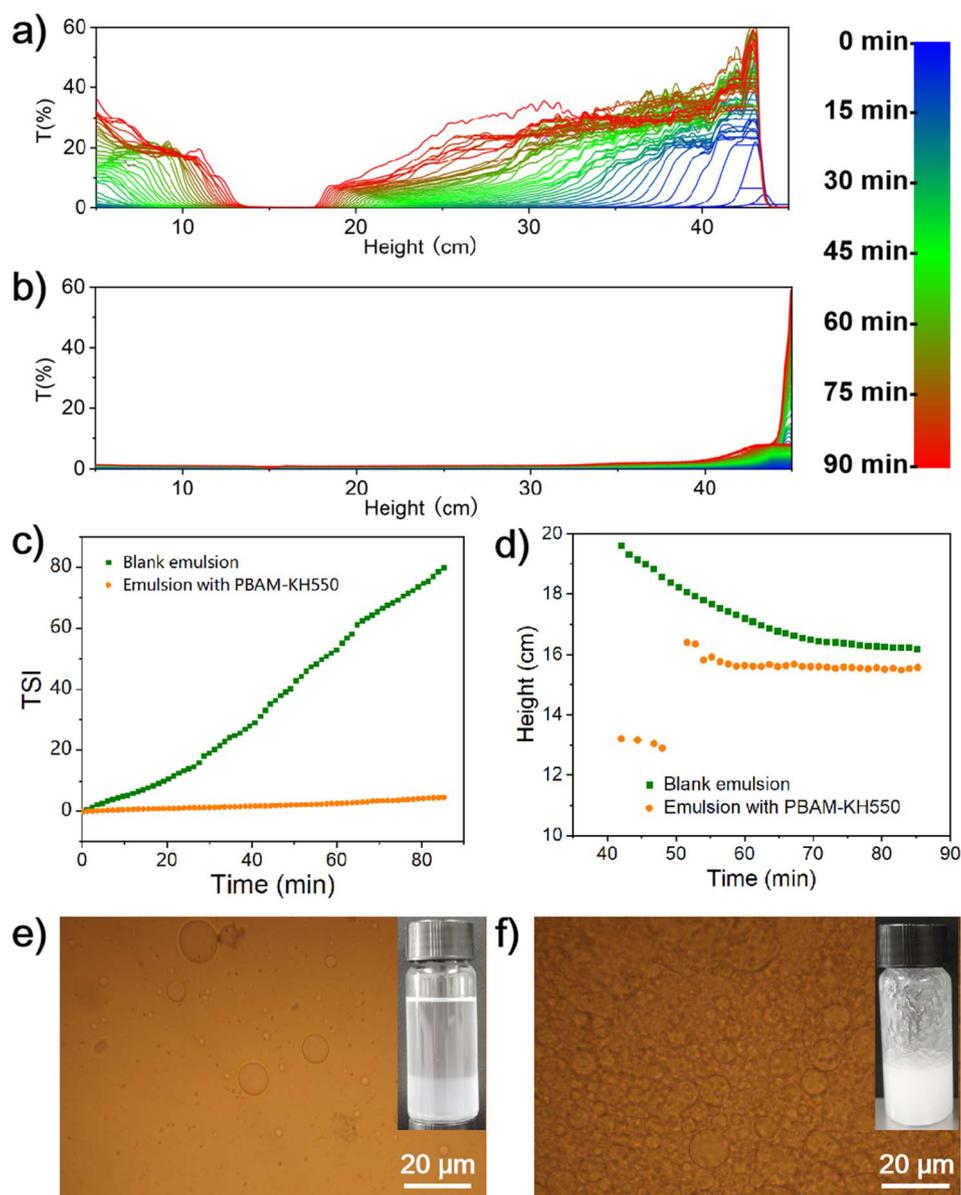

Fig. 11 (a) Stability analyse of the pure silicone oil and DMAc mixture (b) stability analyse of silicone oil and DMAc mixture with PBAM and KH550 (c) TSI data (d) interface migration (e) photomicrograph of the pure silicone oil and DMAc mixture (f) photomicrograph of silicone oil and DMAc mixture with PBAM and KH550.
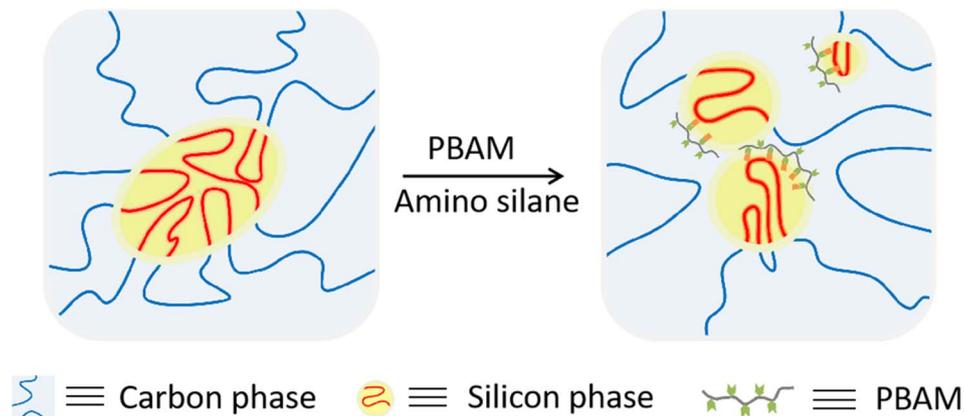
Fig. 12 Microphase separation regulation mechanism diagram of silicone polyurea with PBAM–KH550.

silicone oil. In both cases, the droplets remained stable within the ambient medium. Subsequently, we examined the interfacial interaction between PBAM in DMAc and KH550 in silicone oil. As shown in Fig. 10d, silicone oil droplets were observed to rapidly elongate and deform before detaching. This rapid change is attributed to the reaction between KH550 and PBAM at the interface, which significantly reduced the interfacial tension. This phenomenon confirms the rapid reactivity of PBAM and KH550 at the interface, leading to a sharp decrease in interfacial tension and resulting in the quick detachment of the droplets. This not only demonstrates the ability of PBAM and KH550 to reduce interfacial tension but also suggests that they can exert a similar effect within silicone polyurea materials.

The dispersing and stabilizing effects of PBAM and KH550 in the mixture of silicone and carbon phases were further evaluated. The mixtures of silicone oil and DMAc were stirred at 600 rpm for 30 minutes prior to stability assessment. As depicted in Fig. 11a, the mixture of pure silicone oil and DMAc gradually separated into layers, with an increase in transparency for both phases. This indicates that during the testing process, the two phases were unstable, gradually stratified, and failed to form a stable emulsion. When KH550 and PBAM were introduced into silicone oil and DMAc, respectively, the stability of their mixture was examined, as shown in Fig. 11b. Throughout the entire testing process, no significant changes in translucency was observed in the emulsion formed by DMAc and silicone oil. This demonstrates that the two phases formed a stable emulsion with PBAM and KH550 interfacial action. The TSI values for the emulsion containing PBAM–KH550 were lower than those for the blank emulsion of pure silicone oil and DMAc, as seen in Fig. 11c, further confirming the enhanced stability of the emulsion with PBAM–KH550. After allowing the mixtures to stand for 90 minutes, they were examined under an optical microscope. The blank emulsion of pure silicone oil and DMAc showed almost no stable droplets, as indicated in Fig. 11e. In contrast, the addition of PBAM and KH550 resulted in a large number of emulsion droplets visible in the field of view, as shown in Fig. 11f. Experimental results demonstrate that the interfacial interaction between KH550 and PBAM effectively reduces interfacial tension. This mechanism not only

minimizes the dispersion size of the silicone phase within the carbon matrix but also significantly enhances the dispersion stability of the composite system through improved phase compatibility.

Based on the study findings regarding the dispersing and stabilizing effects of PBAM and KH550 in the mixture of silicone and carbon phases, we propose the mechanism by which KH550 and PBAM reduce the micro-phase separation and enhance tensile properties of silicone polyureas, as illustrated in Fig. 12. Compared with isocyanate and macro-molecular silanes in polyurea, PBAM has more reaction sites, and KH550 has a smaller molecular weight, which makes it easier to react at interface, thereby reducing interfacial tension. Thus, the incorporation of PBAM and KH550 in silicone polyurea leads to the formation of smaller and more stable microscopic phase domains. In addition to this, the product of these interfacial reactions, PBAM–KH550, has both carbon and silicon chains, which strengthens the interfacial adhesion. Consequently, this enhancement in interfacial interaction results in improved mechanical properties of the silicone polyurea.

4   Conclusions

In this paper, the structure and thermal decomposition properties of silicone polyureas we synthesized were characterized by FT-IR and TGA. And the effects of siloxane addition and molecular weight on mechanical properties were studied. On this basis, poly(isobutene-*alt*-maleic anhydride) (PBAM) and γ-aminopropyl triethoxysilane (KH550) which can react at interface were introduced into polyurea and siloxane segments to reduce microphase separation and improve mechanical properties. FT-IR spectroscopy confirmed the rapid reaction between the maleic anhydride groups present in PBAM and the amino groups in KH550. The pendant-drop method demonstrated that the swift interaction at the interface between PBAM and KH550 led to a rapid decrease in interfacial tension. Stability analysis and light microscope observations confirmed that the combination of PBAM and KH550 effectively stabilized the two-phase interface, resulting in the formation of stable droplets within the mixture. SEM revealed a reduction in the degree of

microphase separation within the silicone polyurea. The integration of PBAM and KH550 has been observed to diminish both interfacial tension and particle dispersion size, consequently reducing microphase separation and enhancing the mechanical properties of silicone polyurea.

Data availability

The data that support the findings of this study are available from the corresponding author upon reasonable request.

Author contributions

Yanru Chen: conceptualization, data curation, methodology, project administration, supervision, writing – original draft; Ke Yang: formal analysis; Hanhai Dong: methodology, data curation; Hongyu Niu: methodology; Quanguo Wang: writing – review and editing; Qingli Cheng: writing – review and editing.

Conflicts of interest

There are no conflicts to declare.

References

1 J. Li, W. Jiao, H. Jin, H. Sun, Y. Jia, Z. Chen and X. He, *Chem. Eng. J.*, 2024, **498**, 155793.
2 H. Guo, Y. Sun, Y. Xiao and Y. Chen, *Structures*, 2024, **69**, 107446.
3 J. Xie, H. Pan, Z. Feng, T. Zhen, C. Jiang, Y. Jiang and X. Li, *Int. J. Impact Eng.*, 2025, **195**, 105120.
4 N. Iqbal, P. K. Sharma, D. Kumar and P. K. Roy, *Constr. Build. Mater.*, 2018, **175**, 682–690.
5 L. Wang, J. Zhang, F. Sun, T. Liu, Q. Wang, T. Zhang, J. Xu and J. Fu, *Corros. Sci.*, 2024, **240**, 112395.
6 J. He, X. Sun, D. Pi, X. Wang, M. Wu, W. Qin, A. Wu, Y. Qu and B. Wang, *Constr. Build. Mater.*, 2024, **435**, 136915.
7 P. Xu, S. Yang, R. Yang, R. Wang, G. Chen, Q. Li and Z. Zhou, *Polymer*, 2024, **298**, 126879.
8 Y. Gao, S. Li, S. He, X. Gu, Y. Yue, Y. Chen, H. Zou, Z. Xing and Q. Liu, *Prog. Org. Coat.*, 2024, **192**, 108503.
9 X. Li, F. Bian, R. Huang, J. Wei, X. Gui, J. Hu and S. Lin, *Eur. Polym. J.*, 2024, **221**, 113582.
10 P. Li, Y. Xu, F. Zhang, S. Ren, B. Shi, M. Ning, H. Ma, J. Li and W. Sun, *Colloids Surf., A*, 2024, **694**, 134155.
11 X. Han, W. Zheng, J. Hao, H. Wang, L. Zhu and C. Zhou, *Compos. Commun.*, 2024, **51**, 102082.
12 S. Du, H. Yan, Z. Liu, A. Tang and Y. Li, *J. Mater. Sci. Technol.*, 2023, **151**, 219–226.
13 H. Wang, R. Chen, D. Song, G. Sun, J. Yu, Q. Liu, J. Liu, J. Zhu, P. Liu and J. Wang, *J. Colloid Interface Sci.*, 2024, **653**, 971–980.
14 Z. Sun, J. Wen, W. Wang, H. Fan, Y. Chen, J. Yan and J. Xiang, *Prog. Org. Coat.*, 2020, **146**, 105744.
15 X. Xu, T. Xiao, J. Wen, J. Li, Y. Chen, A. Lu, H. Tan and C. Tang, *Chem. Eng. J.*, 2024, **488**, 150810.
16 B. Qin and J. Xia, *Eur. Polym. J.*, 2024, **219**, 113392.
17 I. Yilgör, E. Yilgör and G. L. Wilkes, *Polymer*, 2015, **58**, A1–A36.
18 Q. Guo, Y. Zhang, Y. Liu and Y. Zhang, *Prog. Org. Coat.*, 2025, **200**, 108989.
19 D. Tyagi, I. Yílgör, J. E. McGrath and G. L. Wilkes, *Polymer*, 1984, **25**, 1807–1816.
20 W. R. Jiang, R. Y. Bao, W. Yang, Z. Y. Liu, B. H. Xie and M. B. Yang, *Mater. Des.*, 2014, **59**, 524–531.
21 S. Pak, S. Park, Y. S. Song and D. Lee, *Compos. Struct.*, 2018, **193**, 73–79.
22 J. B. Olivato, M. V. E. Grossmann, F. Yamashita, D. Eiras and L. A. Pessan, *Carbohydr. Polym.*, 2012, **87**, 2614–2618.
23 X. Zhang, X. Li, G. Ji, J. Huang, T. Li, B. Xia, S. Wang and W. Dong, *Polymer*, 2024, **313**, 127715.
24 P. Singh, P. Katiyar and H. Singh, *Mater. Today: Proc.*, 2023, **78**, 189–197.
25 M. Baron, M. D. Rakotorinina, M. I. El Assil, Y. Guillaneuf, D. Gigmes, D. Siri, A. Gaudel-Siri, J. J. Flat, S. Quinebeche, P. Cassagnau and E. Beyou, *Mater. Today Commun.*, 2019, **19**, 271–276.
26 T. A. Lin, J. H. Lin and L. Bao, *J. Cleaner Prod.*, 2021, **279**, 123473.
27 I. Belyamani, S. Bourdon, J. M. Brossard, L. Cauret, L. Fontaine, V. Montembault and J. Maris, *Waste Manag.*, 2024, **178**, 301–310.
28 S. H. Kameshwari Devi and H. Siddaramaiah, *Mater. Today: Proc.*, 2021, **46**, 2510–2514.
29 X. Hao, J. Xu, H. Zhou, W. Tang, W. Li, Q. Wang and R. Ou, *Mater. Des.*, 2021, **212**, 110182.
30 Y. Chen, R. Wu, J. Zhou, H. Chen and Y. Tan, *Colloids Surf., A*, 2021, **626**, 127004.
31 Y. Chen, Q. Song and Y. Tan, *Colloids Surf., A*, 2022, **348**, 118011.